https://doi.org/10.5194/tc-2021-374
Preprint. Discussion started: 10 January 2022

The Cryosphere Discussions

Filling and drainage of a subglacial lake beneath the Flade Isblink ice cap, northeast Greenland

Qi Liang[1], Wanxin Xiao[1], Ian Howat[2,3], Xiao Cheng[1], Fengming Hui[1], Zhuoqi Chen[1], Mi Jiang[1], Lei Zheng[1]

[1]School of Geospatial Engineering and Science, Sun Yat-sen University & Southern Marine Science and Engineering Guangdong Laboratory (Zhuhai), Zhuhai, Guangdong, China
[2]Byrd Polar and Climate Research Center, Columbus, OH, USA
[3]School of Earth Sciences, Ohio State University, Columbus, OH, USA

Correspondence to: Lei Zheng (zhenglei6@mail.sysu.edu.cn)

Abstract. The generation, transport, storage and drainage of meltwater beneath the ice sheet play important roles in the Greenland ice sheet (GrIS) system. Active subglacial lakes, common features in Antarctica, have recently been detected beneath GrIS and may impact ice sheet hydrology. Despite their potential importance, few repeat subglacial lake filling and drainage events have been identified under Greenland Ice Sheet. Here we examine the surface elevation change of a collapse basin at the Flade Isblink ice cap, northeast Greenland, which formed due to sudden subglacial lake drainage in 2011. We estimate the subglacial lake volume evolution using multi-temporal ArcticDEM data and ICESat-2 altimetry data acquired between 2012 and 2021. Our long-term observations show that the subglacial lake was continuously filled by surface meltwater, with basin surface rising by up to 55 m during 2012-2021 and we estimate 138.2×10^6 m^3 of meltwater was transported into the subglacial lake between 2012 and 2017. A second rapid drainage event occurred in late August 2019, which induced an abrupt ice dynamic response. Comparison between the two drainage events shows that the 2019 drainage released much less water than the 2011 event. We conclude that multiple factors, e.g., the volume of water stored in the subglacial lake and bedrock relief, regulate the episodic filling and drainage of the lake. By comparing the surface meltwater production and the subglacial lake volume change, we find only ~64% of the surface meltwater successfully descended to the bed, suggesting potential processes such as meltwater refreezing and firn aquifer storage, need to be further quantified.

1 Introduction

The Greenland Ice Sheet (GrIS) has experienced a strong negative mass balance since the 1990s (Shepherd et al., 2020). Mass loss has resulted from a combination of increased dynamic thinning (Enderlin et al., 2014; King et al., 2020) and decreased surface mass balance (SMB) (Fettweis et al., 2017; Noël et al., 2019). Of these, the decline in SMB due to an increase in surface melting and runoff has recently become the dominant contributor (Lenaerts et al., 2019). Moreover, the higher runoff may also lead to ice sheet dynamic changes (Hewitt, 2013; van de Wal et al., 2015). Meltwater draining into the englacial system can be accumulated in crevasses and raise the ice temperature, leading to increases in ice velocities due

https://doi.org/10.5194/tc-2021-374
Preprint. Discussion started: 10 January 2022

The Cryosphere Discussions
Open Access
EGU

to the weaken/soften of the ice sheet (Cavanagh et al., 2017; Liang et al., 2019; Phillips et al., 2013). When meltwater penetrates from the surface to the ice sheet bed, it can lubricate the ice bed interface, reduce basal drag and increase glacier sliding (Joughin et al., 2013; Moon et al., 2014; Zwally et al., 2002). Therefore, the presence and movement of meltwater at the ice bed interface are considered to significantly affect ice dynamics (Meierbachtol et al., 2013). Given the expected increases in surface meltwater production in a warming climate (Mottram et al., 2017; Sellevold and Vizcaino, 2021), it is of critical importance to understand the GrIS hydrology, especially the routing, storage, drainage and recharge of subglacial water in Greenland.

Until recently, more than 50 subglacial lakes have been identified beneath the GrIS from airborne radio-echo sounding (Bowling et al., 2019). Most of them are stable lakes located above the Equilibrium Line Altitude (ELA) but away from the ice sheet interior (Bowling et al., 2019), while only a few hydrologically-active lakes that are recharged by surface meltwater have been identified from ice surface elevation change measurements (Bowling et al., 2019; Howat et al., 2015; Livingstone et al., 2019; Palmer et al., 2015; Willis et al., 2015). Compared to the widely distributed stable subglacial lakes, the active subglacial lakes are affected more directly by surface meltwater and their drainage would significantly influence the glacier flow dynamics (Davison et al., 2020; Livingstone et al., 2019). Despite this importance, our understanding of subglacial lakes under GrIS has been primarily developed from theoretical studies or inferences from geophysical exploration due to the limited direct observations (Davison et al., 2019). Remote sensing techniques have recently been used to monitor the subglacial lakes, but few studies have investigated the long-term filling and drainage of subglacial lakes. In particular, the subglacial lake volume change, water residence times and drainage are still poorly understood.

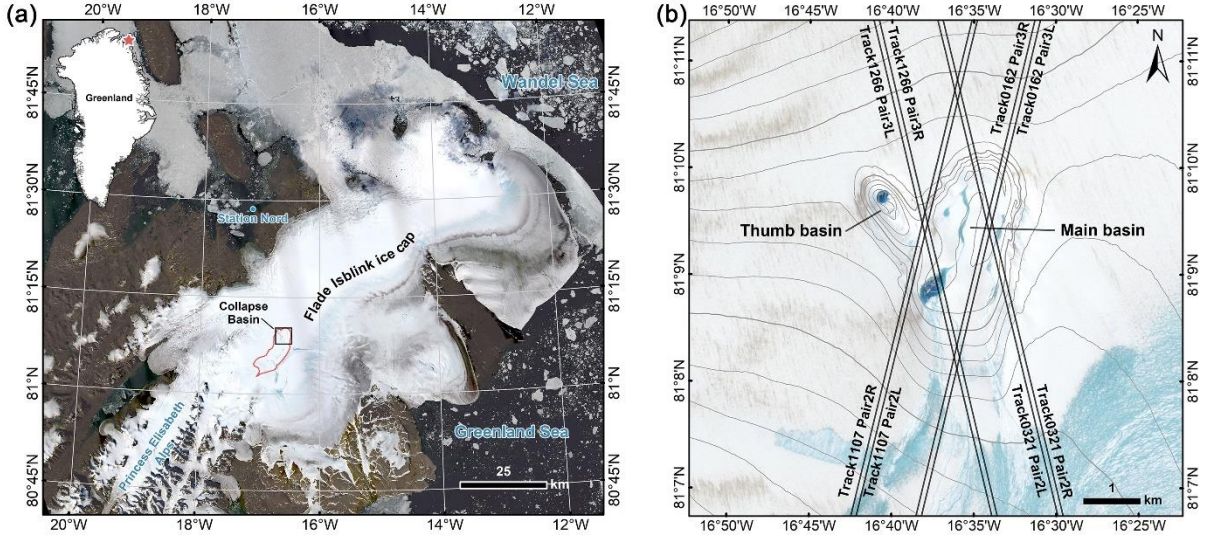

Figure 1. Map of the study area. (a) Flade Isblink ice cap. Background is Landsat-8 OLI image acquired on 13 August 2015. The black box shows location of (b). The red line is catchment boundary. (b) Sentinel-2 MSI image of the deep basin acquired on 5 August 2020. The grey 10-meter contours are derived from ArcticDEM strips data from 20 April 2015. Blue lines indicate the 4 pairs of ICESat-2 single-beam tracks that pass through the collapse basin. The supraglacial meltwater formed in summer usually flows northwards and drains into the ice sheet through crevasses and moulins.

https://doi.org/10.5194/tc-2021-374
Preprint. Discussion started: 10 January 2022

At the Flade Isblink ice cap (81.3°N, 15.0°W) in northeast Greenland (Figure 1), a collapse basin about 70 m deep caused by sudden subglacial lake drainages between August 16 and September 6 in 2011 was first revealed by (Willis et al., 2015). Basin surface elevation estimates with DEMs created from stereoscopic satellite imagery suggest that rapid surface uplift occurred over the two years following the collapse, as supraglacial meltwater transported to the ice base and refilled the subglacial lake. Although this subglacial lake is under the ice cap rather than the wider GrIS, it is important to investigate its behavior and influence due to the similar glacial settings as the GrIS. In order to better understand the repeat subglacial lake filling and drainage, here we extended the surface elevation time series records to early 2021 with ArcticDEM strips data and ICESat-2 altimetry data. We describe the long-term subglacial lake behavior, analyze its volume change and compare it with the surface runoff supply. We also identify a second drainage event in 2019 and explore the impact of drainage on glacier dynamics.

2 Data and method

2.1 Surface elevation and basin volume change calculation

Surface elevations from 2012 to 2017 were first acquired from multi-temporal ArcticDEM strip data (Porter et al., 2018). The initial absolute accuracy of ArcticDEM strip data is less than 4 meters in horizontal and vertical planes. Therefore, the DEM strips should be vertically co-registered before calculating elevation changes. Only a few DEM strips extend over bedrock or have ICESat footprints as ground control points in our study area, so we cannot directly co-register each of them. Instead, we first co-registered a DEM acquired on 20 April 2015 using the 3-dimensional offset values provided by the metadata text file as a reference. A ~7.6×7.6 km window that centered at the collapse basin and with size twice the length and width of the basin was set. Another 800 m buffer was set outward along the boundary of the collapse basin. Then, all the other DEMs were vertically co-registered to the reference DEM by calculating the mean elevation differences using the pixels within this window but outside the 1500-m buffer. We applied an iterative, 3-standard-deviation filter to remove outliers when estimating the elevation differences (Willis et al., 2015). The DEM precision was estimated from the standard deviation of the elevation differences that remained after the iterative filter. In this way, the influence of both the systematic vertical offsets and snow accumulation or melting were removed.

Besides ArcticDEM data, Advanced Land Observing Satellite (ALOS) Global Digital Surface Model "ALOS World 3D" (AW3D30) (Tadono et al., 2014; Takaku et al., 2014, 2020) was also used to analyze the elevation change. The AW3D30 DEM in our study area is derived from data spanning the period 2006–2010, just before late summer of 2011 when the deep basin formed. As above, the AW3D30 DEM was vertically co-registered to the reference DEM. Note that, all the final registered DEMs only represent 'relative' ice surface heights that have eliminated snow depth variation, rather than the true accurate elevation.

The surface elevation measurements from the Advanced Topographic Laser Altimeter System (ATLAS) onboard ICESat-2 were also used to extend the time series to early 2021. As a successor to the ICESat-1 satellite mission, ICESat-2, a polar-

https://doi.org/10.5194/tc-2021-374
Preprint. Discussion started: 10 January 2022

orbiting satellite with 91-day repeat cycle and 92° orbit inclination, was launched in September 2018 (Markus et al., 2017). ATLAS generates six green (532 nm) laser beams in three pairs along one reference ground track and each pair contains one weak and one strong beam. In across-track direction, the spacing between each beam pair is ~3.3 km and the beams within a pair are separated by ~90 m. There are 8 tracks (4 pairs) pass through the collapse basin, with two pairs (Track 0126 pair3 and Track 0321 pair2) pass over the main basin and another two pairs (Track 1266 pair3 and Track 1107 pair2) pass over the area between main basin and thumb basin (Figure 1b). We only used repeat cycles 3-9 for our study because the first two cycles of ICESat-2 data are not repeat cycles due to pointing control issues.

The level 3a Land Ice Height (ATL06) data product was used in this study. We applied an initial filtering process to remove the poor-quality elevation measurements caused by clouds or random clustering of background photons based on the ATL06 quality summary flag (Smith et al., 2019). Then a height consistency check process was introduced by calculating the adjacent elevations using the along-track slope parameter and comparing to the original elevations for the two adjacent measurements. Only the data where the difference between original elevations and the estimated elevations were less than 2 m were used (Li et al., 2020). In order to reduce errors introduced by large across-track slopes, we merged the two single-beam track data for the left beam and right beam into one beam pair. A reference track was first calculated by averaging all the single-beam tracks from both left and right ground tracks. Then the elevation of the reference track for each cycle was estimated from the left and right single-beam track data and the across-track slope parameter (Li et al., 2020). This procedure provides four repeat-track observations for elevation change analysis.

After all the ICESat-2 data are co-registered to the reference DEM using the method described above, the time series of elevation change of collapse basin were estimated along the four reference tracks using both the registered ArcticDEM and ICESat-2 data. Additionally, average ice surface elevation changes were also estimated at three reference track crossovers (Figure 2a).

Volume change of the collapse basin through time was estimated by integrating elevation change over the basin area. We expect that this volume change is mainly caused by ice inflow into the basin and subglacial lake filling. Assuming the elevation changes occurring over the 1500-m buffer region correspond to ice flowing into the basin, we calculate the inflow volume by integrating the surface elevation changes over the buffer area (Willis et al., 2015). The volume change of the subglacial lake is then estimated by differencing the basin volume change and ice inflow volume.

2.2 Catchment delineation and surface melting analysis

The catchment boundary is extracted using ArcticDEM surface elevation as follows (Smith et al., 2017; Yang et al., 2019). First, we fill the ArcticDEM surface to create a sink-free DEM raster. Then we identify the flow directions from the slope direction on the partially filled DEM. Finally, the Basin function in ArcGIS software is used to delineate the catchment boundary.

To assess the surface meltwater dynamics, we use estimates of meltwater runoff from the high-resolution Regional Atmospheric Climate Model (RACMO2.3p2) (Noël et al., 2018). Daily runoff produced in the catchment are generated from

https://doi.org/10.5194/tc-2021-374
Preprint. Discussion started: 10 January 2022

120 RACMO2.3p2 that are statistically downscaled to a 1-km horizontal resolution (Noël et al., 2019). The total runoff within catchment is calculated by summing the 1 km grid cells within the catchment boundary. Furthermore, a series of Landsat-8 Operational Land Imager (OLI) and Sentinel-2 MultiSpectral Instrument (MSI) images acquired during 2014-2020 melt season are used to better illustrate the supraglacial lakes and streams.

2.3 Ice velocity estimate

125 We obtain estimates of the ice surface velocity from the MEaSUREs Greenland Monthly Ice Sheet Velocity Mosaics from SAR and Landsat dataset, Version 3 (Joughin et al., 2018). These include monthly surface velocity estimates for the Greenland Ice Sheet and periphery and are posted at a 200 m grid resolution. To examine the surface velocity variations during the drainage event, we extract the velocity time series from 2018 to 2020 for a small region that is located downstream of the collapse basin, shown in Figure 6c.

130 ## 3. Results

3.1 Collapse basin surface elevation change

After the basin surface rose by up to 38m during 2012-2014 (Willis et al., 2015), the elevation of the entire basin continued to increase during the ArcticDEM period (2012-2017) (Figure 2a). The surface of the main basin and thumb basin uplifted by up to 65 m and 50 m, respectively, while the south part of the collapse basin only had a maximum uplift of ~10 m.
135 Figures 2b-e show sequential elevation profiles for four reference tracks across the basin. Over the main basin, profiles AA' and BB' demonstrate that a rapid surface rise of ~20 m occurred and the shape of the basin surface changed between May 2012 and March 2013. After that, the surface elevation increased more gradually by another ~40 m during 2013-2019. The elevation reached its peak value of ~660 m in April 2019, which is just ~25 m lower than the pre-collapse surface derived from AW3D30 DEM (the thick red solid line in Figure 2b-e). The ice surface elevation then showed a sudden decrease in
140 2019, followed by a gradual increase since January 2020. Profiles CC' and DD' show that the elevation changed gradually while the surface maintained approximately the same shape.

https://doi.org/10.5194/tc-2021-374
Preprint. Discussion started: 10 January 2022

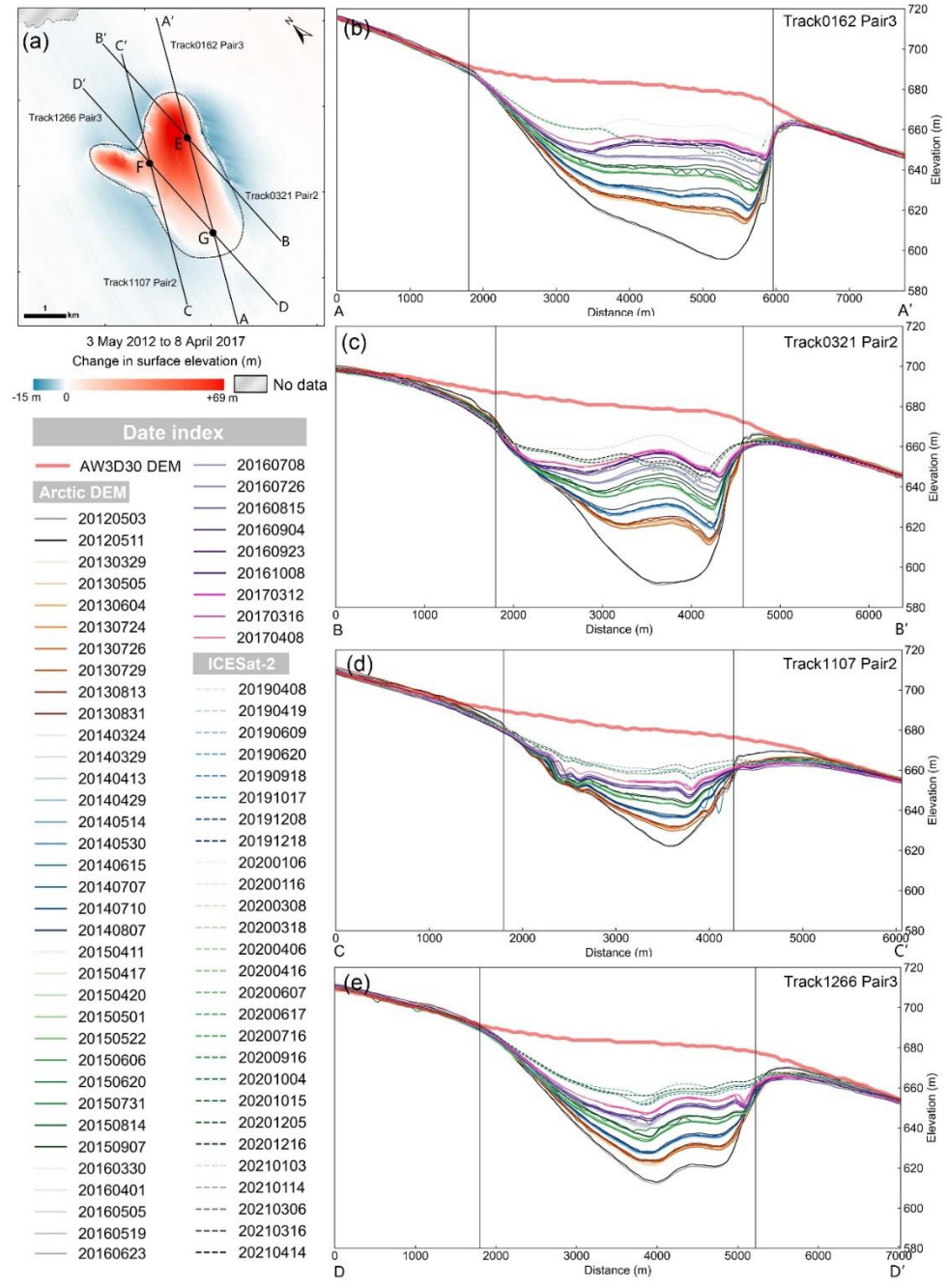

Figure 2. Surface elevation changes from 2012 to 2021. (a) Change in surface elevation between 5 May 2012 and 8 April 2017 (DEM20170408-DEM20120505). The solid lines show the position of the reference track used to extract the elevation profiles. The dashed curve is the boundary of the collapse basin which has an area of about 7.6 km2. The map projection is polar stereographic (EPSG: 3413). (b-e) Repeat elevation profiles derived from ArcticDEM and ICESat-2 data. The start and end of the profile AA', BB', CC' and DD' are shown in (a). Profiles derived from ArcticDEM and ICESat-2 are with solid and dash lines, respectively. The thick red solid line represents the elevation profile derived from AW3D30 DEM which has a timestamp of 2006–2010. The vertical lines demonstrate the position of the collapse basin boundary.

https://doi.org/10.5194/tc-2021-374
Preprint. Discussion started: 10 January 2022

Combining ArcticDEM and ICESat-2 data, we estimate changes in surface elevation at three crossovers (Figure 3). Elevation at the south edge of the collapse basin (crossover G) continuously increased by ~10 m from 2012 to 2021. At the shallow saddle between the main basin and the thumb basin (crossover F), the surface rose at a faster rate of ~5 m/yr during 2012-2021, with a sudden subsidence of ~2 m between 20 June and 18 September in 2019. The main basin (crossover E) had the most rapid surface uplift of ~9 m/yr from May 2012 to April 2019. After continuously increasing for the 8-years after the basin first collapsed in 2011, the surface of the main basin subsided by more than 10 m between 19 April 2019 and 16 January 2020. Afterward, the elevation increased again at rate of ~5 m/yr. The elevation increased dramatically in the melt season during 2014-2016 (Figure 3 inset). During the melt season in 2014 and 2015, the surface of the main basin rose ~3 m at a rate of ~33 m/yr and ~28 m/yr, respectively. In 2016, the elevation gained ~7 m between 8 July and 4 September. The rate of elevation increase of ~49 m/yr is about half of the observed rapid surface uplift during the two-week period in 2012 (Willis et al., 2015).

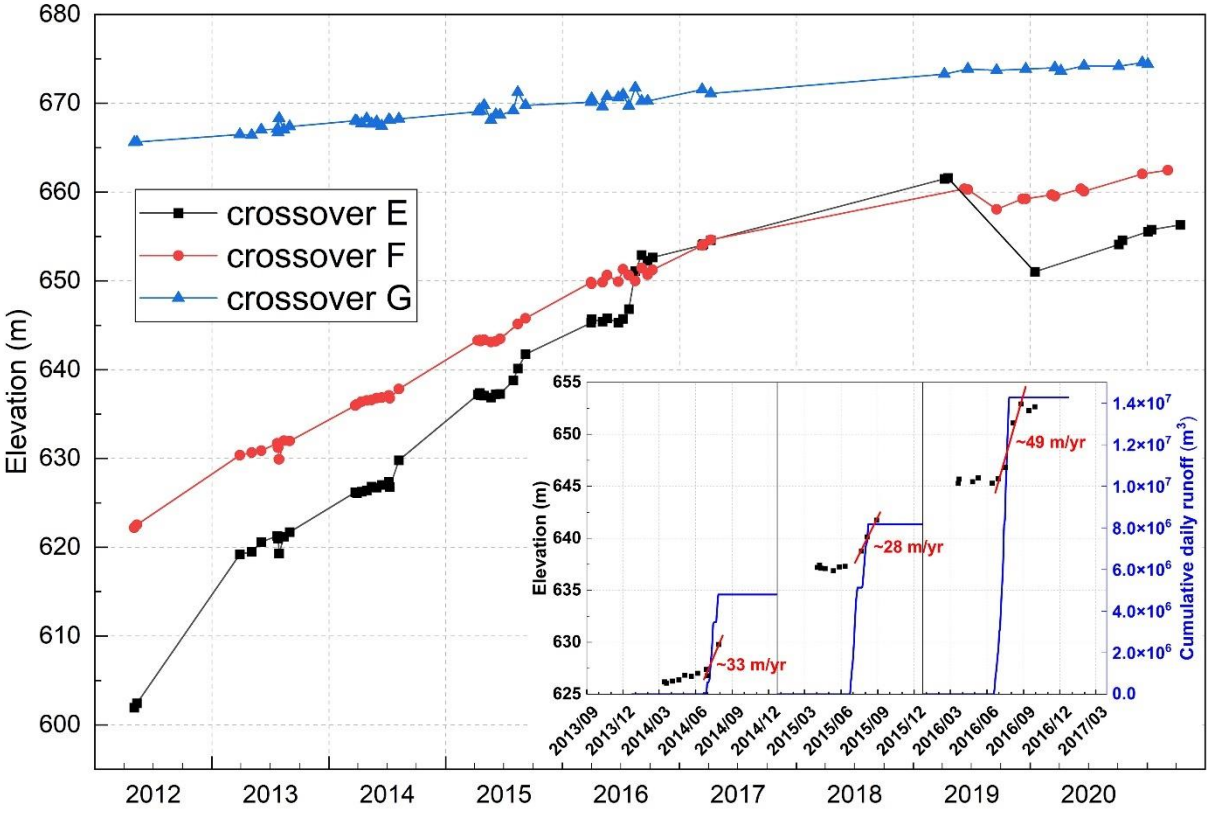

Figure 3. Ice surface elevation change from 2012 to 2021 at the three ICESat-2 crossovers shown in Fig. 2a. Crossover E demonstrates elevation change at the main basin. Crossover F demonstrates elevation change at the shallow saddle between the main basin and the thumb basin. Crossover G demonstrates elevation change at the south edge of the collapse basin. Inset showing enlarged elevation changes during 2014-2016 at Crossover E. Red lines indicate the dramatically elevation increases at each year. The blue lines show the cumulative catchment runoff from RACMO2.3p2 model.

https://doi.org/10.5194/tc-2021-374
Preprint. Discussion started: 10 January 2022

3.2 Subglacial lake volume change and surface meltwater runoff

Time series of volume change of the collapse basin and subglacial lake during the period of 2012-2017 are shown in Figure 4. Between 3 May 2012 and 5 May 2013, the volume of the collapse basin decreased by 47.5×10^6 m^3, with ~55% (26.3×10^6 m^3) of the changes as a result of surface uplift caused by increasing subglacial lake volume, with the remainder due to rapid infilling by ice flow. Since 2013, however, the rate of ice inflow slowed, and only accounting for a small portion of the basin volume change.

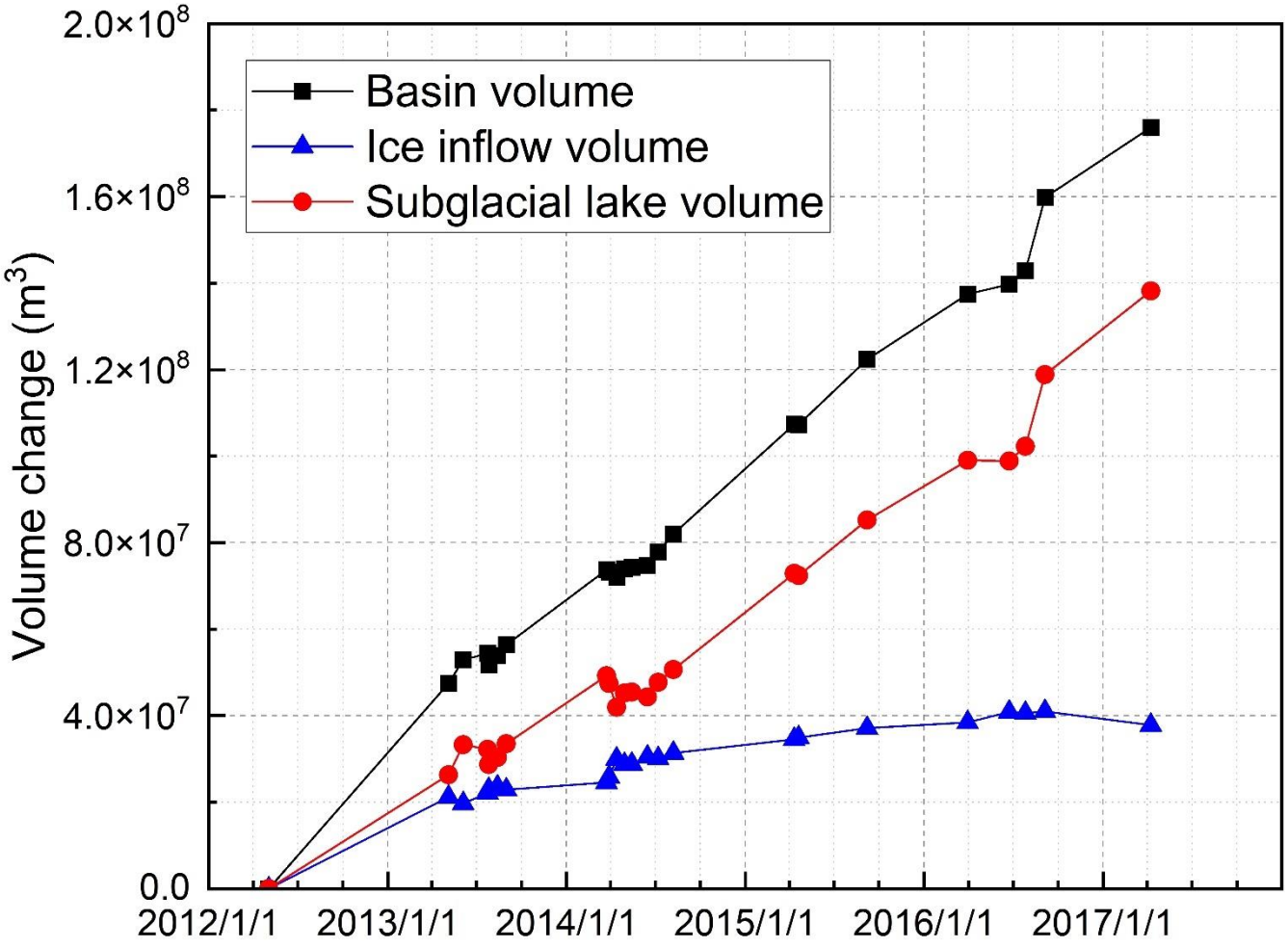

Figure 4. Volume change of collapse basin, ice inflow and subglacial lake relative to 3 May 2012. Volume change of subglacial lake, which is caused by influx of surface meltwater, was derived by differencing the basin volume change and ice inflow volume. DEM with large void in buffer area were discarded to avoid potential bias.

Basin volume showed notable changes corresponding with rapid surface uplift in the 2014-16 melt seasons. In the 2014 melt season, the basin lost a total volume of 4.2×10^6 m^3 between 7 July and 7 August, with the majority of the loss (3.0×10^6 m^3) due to influx of surface meltwater to the subglacial lake. During the 2016 melt season, the volume of the surface basin

https://doi.org/10.5194/tc-2021-374
Preprint. Discussion started: 10 January 2022

decreased by 17.0×10^6 m^3 between 26 July and 4 September, and ~97% (16.6×10^6 m^3) of the volume change was due to subglacial lake refilling. Over the entire 5-year period, the collapse basin lost 176.0×10^6 m^3 of volume. About ~21% (37.8×10^6 m^3) of the loss was due to ice inflow and the remaining, 138.2×10^6 m^3 was the result of subglacial lake refilling by surface meltwater.

4. Discussion

Few active subglacial lakes have been observed under the GrIS (Bowling et al., 2019; Howat et al., 2015; Livingstone et al., 2019; Palmer et al., 2015; Willis et al., 2015). This may be partly because subglacial lakes under GrIS are nearly eight times smaller than in Antarctica (Bowling et al., 2019). Therefore, those subglacial lakes are usually not covered by altimetry observations due to sparse track density at a relatively low polar latitude. Another reason may that the surface of the GrIS margin is typically steeper than in Antarctica, making the depressions in hydraulic potential required for lake formation less likely to occur (Howat et al., 2015). In addition, efficient subglacial drainage systems formed in the melt season may release the stored water, preventing subglacial lake formation. Willis et al. (2015) first discovered the sudden subglacial lake drainage event under Flade Isblink ice cap during the autumn of 2011. As a result, a collapse basin was formed on the surface of the ice cap and the surface rose over the next two years due to recharging of the subglacial lake. Our estimates of the collapse basin and subglacial lake volume change between 3 May 2012 and 5 May 2013 are in agreement with Willis et al. (2015), who reported a similar amount of volume change of 46.5×10^6 m^3 and 29.6×10^6 m^3, respectively. Additionally, we also concur that volume change caused by ice inflow accounted for a large portion of basin volume loss over the first two years (2012-2014) of our investigation period. While as the depression becomes shallower in the following years, less ice would flow into the basin and hence account for little of the basin volume change.

Surface meltwater may drain into crevasses or moulins every melt season and lead to a rapid elevation increase in a short period. Different from the north-flowing meltwater that mainly drained into crevasses on the southern margin of the collapse basin in 2012, the meltwater largely accumulated locally in a supraglacial lake at the southern part of the basin during the 2014-2016 melt season (Figure 5). From the time of surface meltwater draining into moulins and the observed rapid uplift of the main basin in these 3 years, we conclude that surface meltwater recharged the subglacial lake every melt season. Moreover, the larger amount of meltwater observed in 2016 corresponded to larger elevation gains. This may indicate that the subglacial lake volume is primarily controlled by supraglacial meltwater filling.

https://doi.org/10.5194/tc-2021-374
Preprint. Discussion started: 10 January 2022

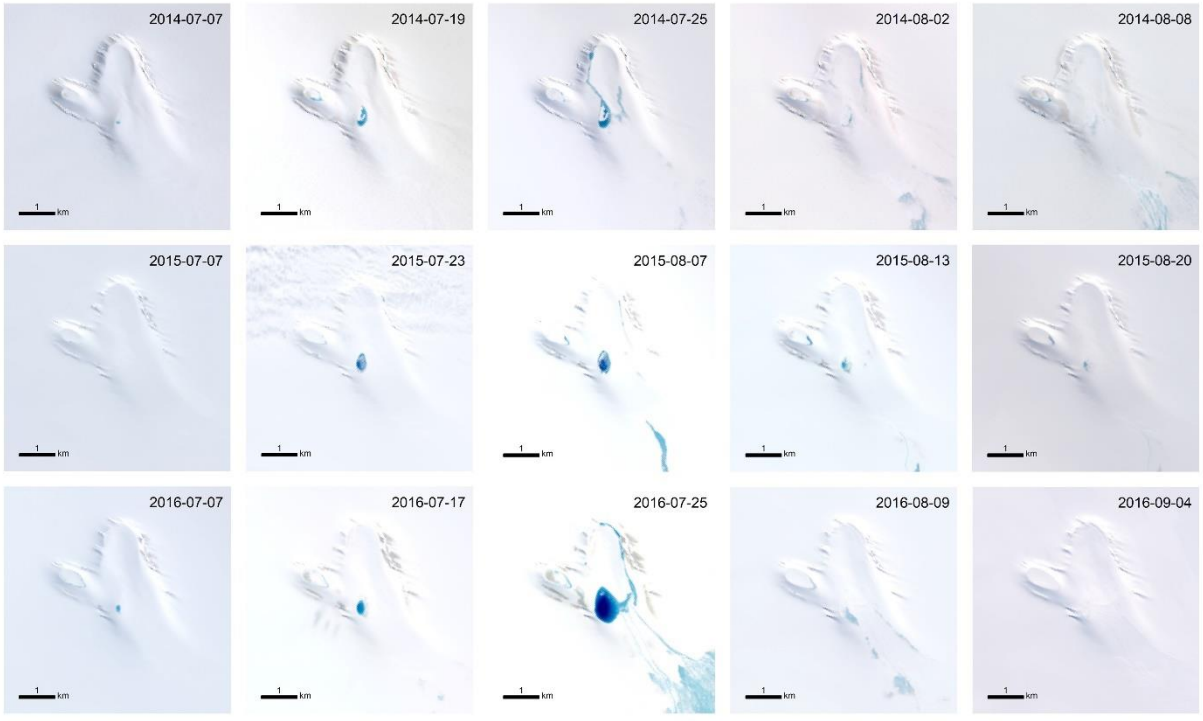

Figure 5. Sequence of Landsat-8 optical imagery showing the surface meltwater evolution during 2014-2016 melt season. Each column from left to right represents different stages of melting.

Between 19 April 2019 and 16 January 2020, the surface of the main basin lowered by more than 10 m (Figure 3). We conclude this surface lowering is most likely due to drainage of the subglacial lake, which is further confirmed by the Sentinel-2 images acquired at the end of August 2019 (Figure 6). Between 24 and 26 August 2019, obvious surface lowering is observed over the main basin and a distinct depression formed at the thumb basin area (Figures 6a-b), indicating a rapid subglacial lake drainage event occurred during this time. Lacking elevation measurements at the main basin in 2019 prevents us from estimating the exact duration of drainage events. While according to the elevation variation at the shallow saddle between the main basin and the thumb basin (crossover F), we speculate the drainage may end in September. The time and duration of this drainage event is consistent with previous large subglacial lake drainage events identified in Greenland (Howat et al., 2015; Livingstone et al., 2019; Palmer et al., 2015; Willis et al., 2015), which usually initiated at a time when subglacial drainage system becomes efficient and meltwater drains through the connected channels (Howat et al., 2015). Additionally, the volume of water drained in the 2019 event would be much less than in 2011, indicating that a large amount of meltwater remained in the subglacial lake.

https://doi.org/10.5194/tc-2021-374
Preprint. Discussion started: 10 January 2022

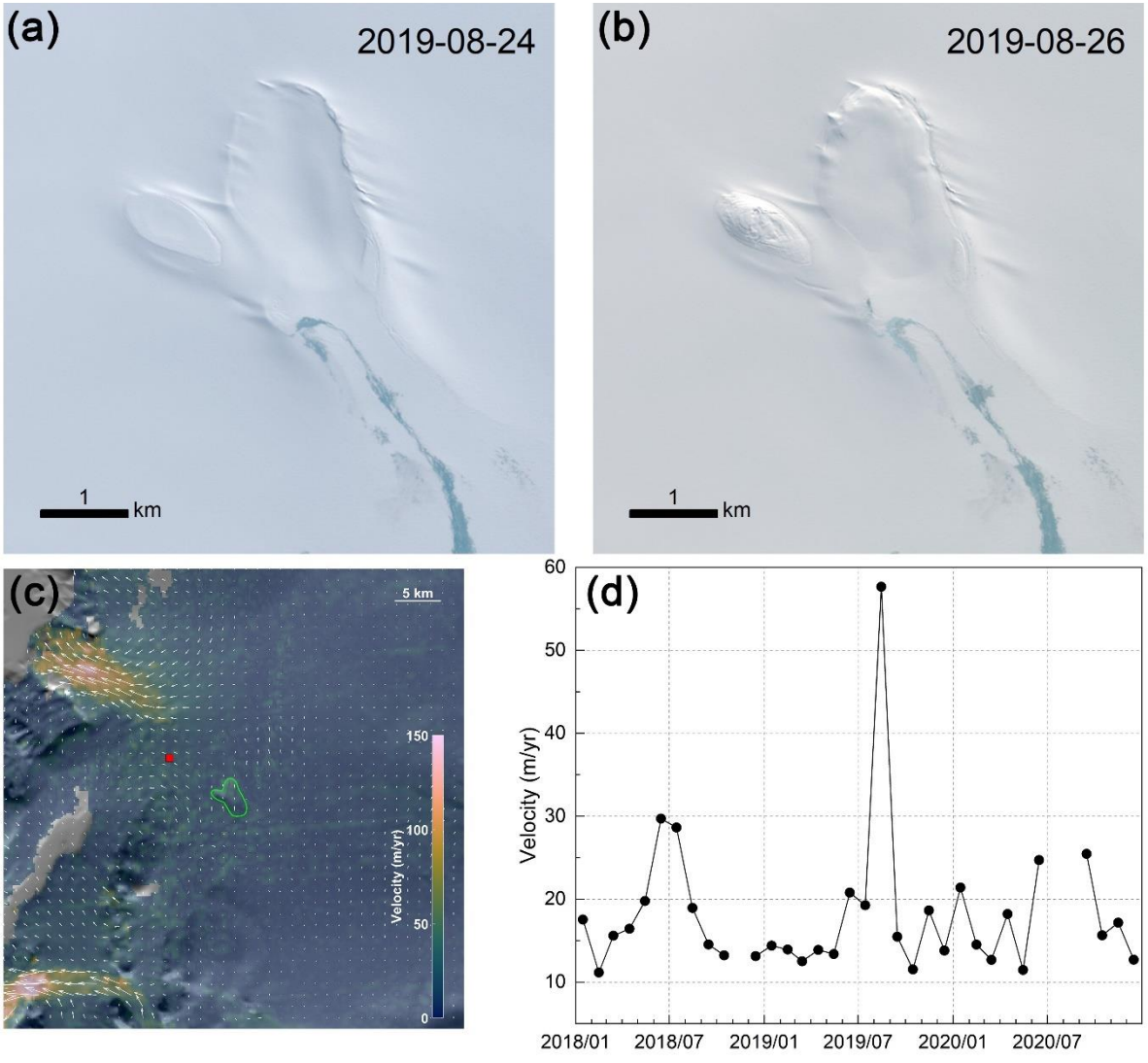

Figure 6. Sentinel-2 optical imagery of the collapse basin and ice surface velocity around it. (a) and (b) are the images showing the obvious surface lowering between 24 and 26 August 2019. (c) The velocity map of September 2019 overlain on MODIS Mosaic of Greenland (MOG) 2015 image maps (Haran et al., 2018). The red square indicates the region of velocity averaging for the velocity time series shown in (d). The green polygon represents the boundary of the collapse basin. The white velocity vectors show direction and magnitude of horizontal velocity. (d) The velocity time series between 2018 and 2020. Each dot represents a monthly average velocity derived from MEaSUREs dataset. Note that data gaps exist due to lack of valid data in that month.

In addition, variations in ice flow speed are consistent with the subglacial lake drainage. In August 2019, ice flow immediately downglacier from the basin increased by a factor of three over the pre-subsidence values (Figure 6d) before decreasing back to average values the following month. We conclude that these abrupt changes resulted from the drainage event, as meltwater released from the subglacial lake initially overwhelmed the drainage system, resulting in a larger

https://doi.org/10.5194/tc-2021-374
Preprint. Discussion started: 10 January 2022

increase in water pressure and sliding speed. As the subglacial drainage system increased in efficiency and/or the discharge of water decreased as the meltwater was drained, water pressures and sliding speeds declined.

The repeat filling and drainage of the subglacial lake is on the scale of ~8 years. Continued basin surface uplift from 2011 to 2019 suggests that the subglacial lake could not be filled by supraglacial meltwater produced in a single melt season and the subglacial lake water storage persists since the collapse basin initially formed. We speculate that, similar to other active subglacial lakes, the subglacial lake may be located upstream of a topographic ridge that would form an area of lower hydropotential and hence could store meltwater draining from the surface (Howat et al., 2015; Palmer et al., 2015). When it has collected sufficient surface meltwater that exceeds the ridge height, the subglacial lake will release all or part of the water through efficient drainage tunnels. Additionally, the elevation profiles through the collapse basin (Figure 2) indicate that the subglacial lake may have not been fully filled when the drainage event occurred in 2019. Similar to other subglacial lakes observed in Greenland (Livingstone et al., 2019), this drainage is also not associated with high surface melt years. All these imply that the repeat filling and drainage is not only decided by the volume of water stored in the subglacial lake, but also may be controlled by meltwater input variability (Schoof, 2010) and bedrock relief (Bowling et al., 2019).

Subglacial lake water beneath the Greenland Ice Sheet is sourced either from geothermal and frictional melting or surface meltwater input (Bowling et al., 2019). The temperature at the bed of Flade Isblink ice cap is far below the pressure melting temperature and the ice moves relatively slowly, ruling out the local production of basal meltwater (Willis et al., 2015). Therefore, surface meltwater is likely the only supply for this subglacial lake. Through crevasses and moulins, the supraglacial meltwater could be routed to the bed and flow towards the ice margin, inducing ice flow variations. A modelling study has estimated that, during an average melt season, about 39% and 47% of the surface runoff are drained through crevasses and moulins in west Greenland, respectively (Koziol et al., 2017). However, only a portion of this surface meltwater would access the ice bed interface (Nienow et al., 2017). Our results show that 3.0×10^6 m^3 of supraglacial water reached the subglacial lake over a one month period (7 July to 7 August) during the 2014 melt season. At the same time, total surface runoff produced within the catchment is estimated to be 4.7×10^6 m^3. Thus, only ~64% of the surface meltwater successfully descended to the bed. The remainder may be refrozen locally in the underlying snowpack (Harper et al., 2012), stored in the firn aquifers (Forster et al., 2014; Kuipers Munneke et al., 2014) or restricted to flow within the firn above ice slabs (MacFerrin et al., 2019).

5. Conclusion

In the autumn of 2011, a collapse basin about 70 m deep formed due to a sudden subglacial lake drainage. Using multi-temporal ArcticDEM and ICESat-2 altimetry data, we document changes in surface elevation of the lake basin and estimate the subglacial lake volume change from 2012 to 2021. The long-term measurements show that the subglacial lake was recharged by surface meltwater produced in the melt season. The surface of the collapse basin rose by up to 55 m over the 9 years, with 138.2×10^6 m^3 of meltwater transported to the subglacial lake during 2012-2017. Our work demonstrates the

https://doi.org/10.5194/tc-2021-374
Preprint. Discussion started: 10 January 2022

potential for subglacial lake to store multi-year meltwater in GrIS, which may affect the ice flow by preventing transfer of meltwater to the ice sheet margin. During our investigation period, a second rapid drainage event occurred in late August 2019, resulting in an abrupt ice velocity change. Compared to the 2011 drainage event, the amount of water drained in 2019 is much smaller and was likely only a portion of the stored water, suggesting partial drainage. In addition, the 2019 drainage was not associated with high surface melt years. These suggest that the triggering of subglacial lake drainage and subsequent evolution may be controlled by multiple factors and need to be further investigated. Furthermore, our study reveals only ~64% of the surface meltwater successfully descended to the bed, implying the importance of quantifying the routing of surface meltwater inputs to the ice bed interface. With the dense tracks of ICESat-2 measurements, more active subglacial lakes under the GrIS will be discovered in the future.

Data availability. ArcticDEM can be obtained from the Polar Geospatial Center (https://www.pgc.umn.edu/data/arcticdem/). ICESat-2 ATL06 data can be obtained from National Snow and Ice Data Center (NSIDC) (https://nsidc.org/data/atl06). MEaSUREs Greenland Monthly Ice Sheet Velocity Mosaics can be obtained from NSIDC (https://nsidc.org/data/NSIDC-0731/versions/3). Landsat-8 images can be obtained from the United States Geological Survey (USGS) (https://earthexplorer.usgs.gov/). Sentinel-2 images can be obtained from the European Space Agency (https://scihub.copernicus.eu/dhus/#/home). AW3D30 DEM can be obtained from the Japan Aerospace Exploration Agency (JAXA) (https://www.eorc.jaxa.jp/ALOS/en/dataset/aw3d30/aw3d30_e.htm). RACMO2.3p2 Greenland daily runoff data were kindly provided by Brice Noël.

Author contributions. QL and LZ conceived the study. WX and QL processed the data and QL wrote the manuscript. All authors contributed to the data analysis and result interpretation.

Competing interests. The authors declare they have no conflict of interest.

Acknowledgements. This research was supported by the National Science Foundation for Distinguished Young Scholars (41925027) and the Innovation Group Project of Southern Marine Science and Engineering Guangdong Laboratory (Zhuhai) (No. 311021008).

References

Bowling, J. S., Livingstone, S. J., Sole, A. J., and Chu, W.: Distribution and dynamics of Greenland subglacial lakes, Nature communications, 10, 2810, 10.1038/s41467-019-10821-w, 2019.

https://doi.org/10.5194/tc-2021-374
Preprint. Discussion started: 10 January 2022

295 Cavanagh, J. P., Lampkin, D. J., and Moon, T.: Seasonal Variability in Regional Ice Flow Due to Meltwater Injection Into the Shear Margins of Jakobshavn Isbræ, J. Geophys. Res. Earth Surf., 122, 2488-2505, 10.1002/2016jf004187, 2017.

Davison, B. J., Sole, A. J., Livingstone, S. J., Cowton, T. R., and Nienow, P. W.: The Influence of Hydrology on the Dynamics of Land-Terminating Sectors of the Greenland Ice Sheet, Front Earth Sci, 7, 10.3389/feart.2019.00010, 2019.

Davison, B. J., Sole, A. J., Cowton, T. R., Lea, J. M., Slater, D. A., Fahrner, D., and Nienow, P. W.: Subglacial Drainage
300 Evolution Modulates Seasonal Ice Flow Variability of Three Tidewater Glaciers in Southwest Greenland, J. Geophys. Res. Earth Surf., 125, e2019JF005492, 10.1029/2019JF005492, 2020.

Enderlin, E. M., Howat, I. M., Jeong, S., Noh, M. J., van Angelen, J. H., and van den Broeke, M. R.: An improved mass budget for the Greenland ice sheet, Geophys. Res. Lett., 41, 866-872, Doi 10.1002/2013gl059010, 2014.

Fettweis, X., Box, J. E., Agosta, C., Amory, C., Kittel, C., Lang, C., van As, D., Machguth, H., and Gallée, H.:
305 Reconstructions of the 1900–2015 Greenland ice sheet surface mass balance using the regional climate MAR model, The Cryosphere, 11, 1015-1033, 10.5194/tc-11-1015-2017, 2017.

Forster, R. R., Box, J. E., van den Broeke, M. R., Miège, C., Burgess, E. W., van Angelen, J. H., Lenaerts, J. T. M., Koenig, L. S., Paden, J., Lewis, C., Gogineni, S. P., Leuschen, C., and McConnell, J. R.: Extensive liquid meltwater storage in firn within the Greenland ice sheet, Nature Geosci., 7, 95-98, 10.1038/ngeo2043, 2014.

310 Haran, T., Bohlander, J., Scambos, T., Painter, T., and Fahnestock, M.: MEaSUREs MODIS Mosaic of Greenland (MOG) 2005, 2010, and 2015 Image Maps, Version 2, National Snow and Ice Data Center [dataset], https://doi.org/10.5067/9ZO79PHOTYE5, 2018.

Harper, J., Humphrey, N., Pfeffer, W. T., Brown, J., and Fettweis, X.: Greenland ice-sheet contribution to sea-level rise buffered by meltwater storage in firn, Nature, 491, 240-243, 10.1038/nature11566, 2012.

315 Hewitt, I. J.: Seasonal changes in ice sheet motion due to melt water lubrication, Earth Planet. Sci. Lett., 371-372, 16-25, https://doi.org/10.1016/j.epsl.2013.04.022, 2013.

Howat, I. M., Porter, C., Noh, M. J., Smith, B. E., and Jeong, S.: Brief Communication: Sudden drainage of a subglacial lake beneath the Greenland Ice Sheet, The Cryosphere, 9, 103-108, 10.5194/tc-9-103-2015, 2015.

Joughin, I., Smith, B. E., and Howat, I.: Greenland Ice Mapping Project: ice flow velocity variation at sub-monthly to
320 decadal timescales, The Cryosphere, 12, 2211-2227, 10.5194/tc-12-2211-2018, 2018.

Joughin, I., Das, S. B., Flowers, G. E., Behn, M. D., Alley, R. B., King, M. A., Smith, B. E., Bamber, J. L., van den Broeke, M. R., and van Angelen, J. H.: Influence of ice-sheet geometry and supraglacial lakes on seasonal ice-flow variability, The Cryosphere, 7, 1185-1192, 10.5194/tc-7-1185-2013, 2013.

King, M. D., Howat, I. M., Candela, S. G., Noh, M. J., Jeong, S., Noël, B. P. Y., van den Broeke, M. R., Wouters, B., and
325 Negrete, A.: Dynamic ice loss from the Greenland Ice Sheet driven by sustained glacier retreat, Communications Earth & Environment, 1, 1, 10.1038/s43247-020-0001-2, 2020.

Koziol, C., Arnold, N., Pope, A., and Colgan, W.: Quantifying supraglacial meltwater pathways in the Paakitsoq region, West Greenland, J. Glaciol., 63, 464-476, 10.1017/jog.2017.5, 2017.

Lenaerts, J. T. M., Medley, B., van den Broeke, M. R., and Wouters, B.: Observing and Modeling Ice Sheet Surface Mass Balance, Reviews of Geophysics, 57, 376-420, 10.1029/2018RG000622, 2019.

Li, T., Dawson, G. J., Chuter, S. J., and Bamber, J. L.: Mapping the grounding zone of Larsen C Ice Shelf, Antarctica, from ICESat-2 laser altimetry, The Cryosphere, 14, 3629-3643, 10.5194/tc-14-3629-2020, 2020.

Liang, Q., Zhou, C., Howat, I. M., Jeong, S., Liu, R., and Chen, Y.: Ice flow variations at Polar Record Glacier, East Antarctica, J. Glaciol., 65, 279-287, 10.1017/jog.2019.6, 2019.

Livingstone, S. J., Sole, A. J., Storrar, R. D., Harrison, D., Ross, N., and Bowling, J.: Brief communication: Subglacial lake drainage beneath Isunguata Sermia, West Greenland: geomorphic and ice dynamic effects, The Cryosphere, 13, 2789-2796, 10.5194/tc-13-2789-2019, 2019.

MacFerrin, M., Machguth, H., As, D. v., Charalampidis, C., Stevens, C. M., Heilig, A., Vandecrux, B., Langen, P. L., Mottram, R., Fettweis, X., Broeke, M. R. v. d., Pfeffer, W. T., Moussavi, M. S., and Abdalati, W.: Rapid expansion of Greenland's low-permeability ice slabs, Nature, 573, 403-407, 10.1038/s41586-019-1550-3, 2019.

Markus, T., Neumann, T., Martino, A., Abdalati, W., Brunt, K., Csatho, B., Farrell, S., Fricker, H., Gardner, A., Harding, D., Jasinski, M., Kwok, R., Magruder, L., Lubin, D., Luthcke, S., Morison, J., Nelson, R., Neuenschwander, A., Palm, S., Popescu, S., Shum, C. K., Schutz, B. E., Smith, B., Yang, Y., and Zwally, J.: The Ice, Cloud, and land Elevation Satellite-2 (ICESat-2): Science requirements, concept, and implementation, Remote Sens. Environ., 190, 260-273, 10.1016/j.rse.2016.12.029, 2017.

Meierbachtol, T., Harper, J., and Humphrey, N.: Basal Drainage System Response to Increasing Surface Melt on the Greenland Ice Sheet, Science, 341, 777-779, doi:10.1126/science.1235905, 2013.

Moon, T., Joughin, I., Smith, B., van den Broeke, M. R., van de Berg, W. J., Noel, B., and Usher, M.: Distinct patterns of seasonal Greenland glacier velocity, Geophys. Res. Lett., 41, 7209-7216, 10.1002/2014GL061836, 2014.

Mottram, R., Boberg, F., Langen, P., Yang, S., Rodehacke, C., Christensen, J. H., and Madsen, M. S.: Surface mass balance of the Greenland ice sheet in the regional climate model HIRHAM5: Present state and future prospects, Low Temperature Science, 75, 105-115, 10.14943/lowtemsci.75.105, 2017.

Munneke, P. K., M. Ligtenberg, S. R., van den Broeke, M. R., van Angelen, J. H., and Forster, R. R.: Explaining the presence of perennial liquid water bodies in the firn of the Greenland Ice Sheet, Geophys. Res. Lett., 41, 476-483, https://doi.org/10.1002/2013GL058389, 2014.

Nienow, P. W., Sole, A. J., Slater, D. A., and Cowton, T. R.: Recent Advances in Our Understanding of the Role of Meltwater in the Greenland Ice Sheet System, Current Climate Change Reports, 3, 330-344, 10.1007/s40641-017-0083-9, 2017.

Noël, B., Berg, W. J. v. d., Lhermitte, S., and Broeke, M. R. v. d.: Rapid ablation zone expansion amplifies north Greenland mass loss, Science Advances, 5, eaaw0123, doi:10.1126/sciadv.aaw0123, 2019.

Noël, B., van de Berg, W. J., van Wessem, J. M., van Meijgaard, E., van As, D., Lenaerts, J. T. M., Lhermitte, S., Kuipers Munneke, P., Smeets, C. J. P. P., van Ulft, L. H., van de Wal, R. S. W., and van den Broeke, M. R.: Modelling the climate

and surface mass balance of polar ice sheets using RACMO2 – Part 1: Greenland (1958–2016), Cryosphere, 12, 811-831, 10.5194/tc-12-811-2018, 2018.

Palmer, S., McMillan, M., and Morlighem, M.: Subglacial lake drainage detected beneath the Greenland ice sheet, Nature communications, 6, 8408, 10.1038/ncomms9408, 2015.

Phillips, T., Rajaram, H., Colgan, W., Steffen, K., and Abdalati, W.: Evaluation of cryo-hydrologic warming as an explanation for increased ice velocities in the wet snow zone, Sermeq Avannarleq, West Greenland, J. Geophys. Res. Earth Surf., 118, 1241-1256, https://doi.org/10.1002/jgrf.20079, 2013.

Porter, C., Morin, P., Howat, I., Noh, M.-J., Bates, B., Peterman, K., Keesey, S., Schlenk, M., Gardiner, J., Tomko, K., Willis, M., Kelleher, C., Cloutier, M., Husby, E., Foga, S., Nakamura, H., Platson, M., Wethington, M., Jr., Williamson, C., Bauer, G., Enos, J., Arnold, G., Kramer, W., Becker, P., Doshi, A., D'Souza, C., Cummens, P., Laurier, F., and Bojesen, M.: ArcticDEM (V1), Harvard Dataverse [dataset], https://doi.org/10.7910/DVN/OHHUKH, 2018.

Schoof, C.: Ice-sheet acceleration driven by melt supply variability, Nature, 468, 803-806, 10.1038/nature09618, 2010.

Sellevold, R. and Vizcaino, M.: First Application of Artificial Neural Networks to Estimate 21st Century Greenland Ice Sheet Surface Melt, Geophys. Res. Lett., 48, e2021GL092449, https://doi.org/10.1029/2021GL092449, 2021.

Shepherd, A., Ivins, E., Rignot, E., Smith, B., van den Broeke, M., Velicogna, I., Whitehouse, P., Briggs, K., Joughin, I., Krinner, G., Nowicki, S., Payne, T., Scambos, T., Schlegel, N., A, G., Agosta, C., Ahlstrøm, A., Babonis, G., Barletta, V. R., Bjørk, A. A., Blazquez, A., Bonin, J., Colgan, W., Csatho, B., Cullather, R., Engdahl, M. E., Felikson, D., Fettweis, X., Forsberg, R., Hogg, A. E., Gallee, H., Gardner, A., Gilbert, L., Gourmelen, N., Groh, A., Gunter, B., Hanna, E., Harig, C., Helm, V., Horvath, A., Horwath, M., Khan, S., Kjeldsen, K. K., Konrad, H., Langen, P. L., Lecavalier, B., Loomis, B., Luthcke, S., McMillan, M., Melini, D., Mernild, S., Mohajerani, Y., Moore, P., Mottram, R., Mouginot, J., Moyano, G., Muir, A., Nagler, T., Nield, G., Nilsson, J., Noël, B., Otosaka, I., Pattle, M. E., Peltier, W. R., Pie, N., Rietbroek, R., Rott, H., Sandberg Sørensen, L., Sasgen, I., Save, H., Scheuchl, B., Schrama, E., Schröder, L., Seo, K.-W., Simonsen, S. B., Slater, T., Spada, G., Sutterley, T., Talpe, M., Tarasov, L., van de Berg, W. J., van der Wal, W., van Wessem, M., Vishwakarma, B. D., Wiese, D., Wilton, D., Wagner, T., Wouters, B., Wuite, J., and The, I. T.: Mass balance of the Greenland Ice Sheet from 1992 to 2018, Nature, 579, 233-239, 10.1038/s41586-019-1855-2, 2020.

Smith, B., Fricker, H. A., Holschuh, N., Gardner, A. S., Adusumilli, S., Brunt, K. M., Csatho, B., Harbeck, K., Huth, A., Neumann, T., Nilsson, J., and Siegfried, M. R.: Land ice height-retrieval algorithm for NASA's ICESat-2 photon-counting laser altimeter, Remote Sens. Environ., 233, 111352, https://doi.org/10.1016/j.rse.2019.111352, 2019.

Smith, L. C., Yang, K., Pitcher, L. H., Overstreet, B. T., Chu, V. W., Rennermalm, A. K., Ryan, J. C., Cooper, M. G., Gleason, C. J., Tedesco, M., Jeyaratnam, J., van As, D., van den Broeke, M. R., van de Berg, W. J., Noel, B., Langen, P. L., Cullather, R. I., Zhao, B., Willis, M. J., Hubbard, A., Box, J. E., Jenner, B. A., and Behar, A. E.: Direct measurements of meltwater runoff on the Greenland ice sheet surface, Proc. Natl. Acad. Sci. USA, 114, E10622-E10631, 10.1073/pnas.1707743114, 2017.

Tadono, T., Ishida, H., Oda, F., Naito, S., Minakawa, K., and Iwamoto, H.: Precise Global DEM Generation by ALOS PRISM, ISPRS Annals of the Photogrammetry, Remote Sensing and Spatial Information Sciences, II-4, 71-76, 10.5194/isprsannals-II-4-71-2014, 2014.

Takaku, J., Tadono, T., and Tsutsui, K.: Generation of High Resolution Global DSM from ALOS PRISM, The International Archives of the Photogrammetry, Remote Sensing and Spatial Information Sciences, XL-4, 243-248, 10.5194/isprsarchives-XL-4-243-2014, 2014.

Takaku, J., Tadono, T., Doutsu, M., Ohgushi, F., and Kai, H.: UPDATES OF 'AW3D30' ALOS GLOBAL DIGITAL SURFACE MODEL WITH OTHER OPEN ACCESS DATASETS, The International Archives of the Photogrammetry, Remote Sensing and Spatial Information Sciences, XLIII-B4-2020, 183-189, 10.5194/isprs-archives-XLIII-B4-2020-183-2020, 2020.

van de Wal, R. S. W., Smeets, C. J. P. P., Boot, W., Stoffelen, M., van Kampen, R., Doyle, S. H., Wilhelms, F., van den Broeke, M. R., Reijmer, C. H., Oerlemans, J., and Hubbard, A.: Self-regulation of ice flow varies across the ablation area in south-west Greenland, The Cryosphere, 9, 603-611, 10.5194/tc-9-603-2015, 2015.

Willis, M. J., Herried, B. G., Bevis, M. G., and Bell, R. E.: Recharge of a subglacial lake by surface meltwater in northeast Greenland, Nature, 518, 223-227, 10.1038/nature14116, 2015.

Yang, K., Smith, L. C., Fettweis, X., Gleason, C. J., Lu, Y., and Li, M.: Surface meltwater runoff on the Greenland ice sheet estimated from remotely sensed supraglacial lake infilling rate, Remote Sens. Environ., 234, 111459, https://doi.org/10.1016/j.rse.2019.111459, 2019.

Zwally, H. J., Abdalati, W., Herring, T., Larson, K., Saba, J., and Steffen, K.: Surface melt-induced acceleration of Greenland ice-sheet flow, Science, 297, 218-222, DOI 10.1126/science.1072708, 2002.